

## **Thermal Conductivity of Difluoromonochloromethane in the Critical Region**

**O. B. Tsvetkov<sup>1</sup> and Y. A. Lapyev<sup>1</sup>**

*Received January 23, 1990*

---

The thermal conductivity of difluoromonochloromethane (refrigerant R22) has been measured along six near-critical isotherms at reduced temperatures varying from  $\tau = 1.005$  to  $\tau = 1.112$  and at pressures ranging from 2.0 to 9.5 MPa. An anomalous enhancement of the thermal conductivity has been observed in the critical region. This anomalous behavior is consistent with theoretical predictions and equations for the thermal conductivity as a function of density and temperature are presented.

---

**KEY WORDS:** critical phenomena; difluoromonochloromethane; refrigerants; R22; thermal conductivity.

### **1. INTRODUCTION**

Refrigerant R22 ( $\text{CHF}_2\text{Cl}$ ), a saturated halogen derivative of methane, is the most commonly used working fluid employed in refrigerating machines. Experimental data for the thermal conductivity of R22 reported before 1975 have been thoroughly analyzed in some standard references [1, 2]. The present paper reports new experimental results for the thermal conductivity of R22, including measurements in the critical region. Representative equations for the thermal conductivity have been derived on the basis of the present data as well as those of the other workers [3–5] not incorporated in the standard references mentioned above [1, 2].

### **2. EXPERIMENTAL**

The thermal-conductivity measurements were obtained with the steady-state variant of the method of coaxial cylinders. The inner copper

---

<sup>1</sup> Leningrad Technological Institute of the Refrigeration Industry, 191002 Leningrad, USSR.

cylinder had a diameter of 14.670 mm and a height of 108.00 mm. The outer cylinder had an inner diameter of 15.110 mm and a mass exceeding 20 kg. A description of the apparatus and the measurement procedure can be found in an earlier publication [6].

In order to validate the reliability of the experimental method, test measurements were made of the thermal conductivity of carbon dioxide in the critical region. The results obtained for carbon dioxide were compared with the thermal conductivity data obtained earlier at the Van der Waals Laboratory with a parallel-plate apparatus [7, 8]. In such a parallel-plate apparatus, the conditions for avoiding convection in the critical region are more favorable than in a coaxial-cylinder apparatus. A comparison of our thermal conductivity data for  $\text{CO}_2$  near the critical temperature ( $T_c = 304.107 \text{ K}$ ) with the literature data [7, 8] is presented in Fig. 1. The measurements were obtained for various temperature differences across the annular fluid layer between the two coaxial cylinders. The results presented in Fig. 1 confirm that our experimental method yields qualitatively and quantitatively reliable results for thermal conductivity.

The R22 sample, used in the measurements, was synthesized in the State Institute of Applied Chemistry (GIPKh) and had an original stated purity of 99.95%.

The thermal-conductivity data obtained for R22 are presented in Table I. Plots of the thermal conductivity as a function of pressure are

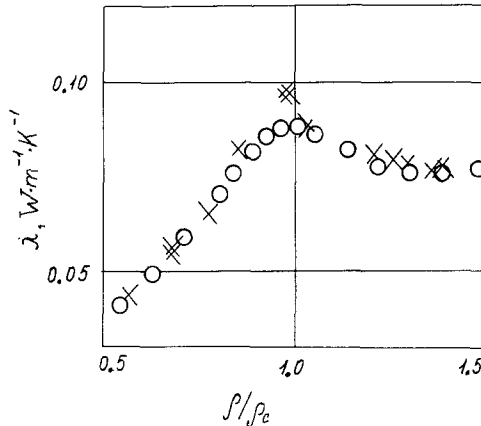


**Fig. 1.** Thermal conductivity of  $\text{CO}_2$  in the critical region as a function of the reduced density  $\rho/\rho_c$ . The circles indicate the data of the Van der Waals Laboratory [7, 8] obtained at  $T = 307.95 \text{ K}$  and the crosses indicate the data obtained with our apparatus at  $T = 308.39 \text{ K}$ .

Table I. Thermal Conductivity of R22

$T$ (K)	P (MPa)	$10^5 \lambda$ (W · m <sup>-1</sup> · K <sup>-1</sup> )	$T$ (K)	P (MPa)	$10^5 \lambda$ (W · m <sup>-1</sup> · K <sup>-1</sup> )
313.45	2.08	7575	366.85	2.00	1697
313.83	4.20	7768	367.71	4.94	4888
316.25	0.80	1232	367.74	5.02	5419
317.99	0.80	1256	368.40	4.99	5874
318.83	4.20	7702	368.43	4.60	2822
319.13	0.10	1178	368.47	5.07	5429
319.51	2.18	7320	368.62	5.10	4918
319.52	0.80	1248	368.77	4.83	4246
323.44	4.76	7398	368.81	4.80	3799
323.44	6.00	7496	369.38	7.30	5689
323.44	6.95	7553	369.55	5.87	5413
326.00	2.56	7080	369.65	5.25	5452
345.50	3.32	6184	370.23	4.98	4738
346.63	2.96	1920	370.24	4.85	3393
355.85	5.20	5985	370.24	4.92	3846
355.87	2.20	1673	370.90	5.90	5408
356.54	0.80	1476	370.93	6.09	5438
357.71	0.10	1430	370.95	5.47	5263
363.73	8.20	6079	370.95	6.29	5470
364.30	5.02	5554	370.97	6.55	5517
365.46	3.10	1880	370.99	5.12	14360
365.80	1.63	1627	371.02	5.10	6241
365.99	7.40	6096	371.05	5.03	11920
371.08	5.11	7123	373.31	5.32	7123
371.08	5.11	7342	373.32	5.75	5260
371.10	4.95	3546	373.35	5.28	5327
371.11	4.90	3331	373.36	5.30	6208
371.11	5.15	11910	373.38	5.24	4584
371.12	4.65	2971	373.38	5.44	6116
371.12	4.80	3053	373.38	6.00	5250
371.13	5.06	4687	373.39	6.45	5333
371.13	5.23	9770	373.40	6.45	5358
371.13	5.15	11760	373.41	5.49	5671
371.13	5.19	6527	373.59	5.00	3240
371.14	5.02	4047	373.72	4.46	2462
371.14	5.16	10900	373.84	3.46	2007
371.16	5.00	3841	374.30	8.41	5696
371.17	5.28	5542	374.34	4.14	2228
371.21	5.15	12630	375.21	0.98	1614
371.29	5.20	7540	376.82	2.85	1895
371.34	5.06	4301	380.50	6.50	5006
371.35	5.20	8149	380.69	6.94	5048
371.52	5.06	4357	380.71	6.50	5002
371.62	5.08	5162	380.72	6.95	5160

Table I. (Continued)

$T$ (K)	P (MPa)	$10^5 \lambda$ (W · m <sup>-1</sup> · K <sup>-1</sup> )	$T$ (K)	P (MPa)	$10^5 \lambda$ (W · m <sup>-1</sup> · K <sup>-1</sup> )
373.24	5.39	6744	380.87	5.90	4516
373.28	5.33	7600	380.87	5.95	4684
373.28	5.42	6414	380.88	5.78	4041
373.28	5.50	5496	380.88	5.99	5036
373.29	5.35	7446	380.89	6.04	4899
373.29	5.35	7492	380.89	6.25	5021
380.90	5.59	3456	396.74	4.74	2297
380.93	4.87	2577	396.75	4.46	2224
384.23	5.31	2755	396.75	5.19	2449
384.23	5.49	2904	396.76	4.64	2265
384.24	5.00	2553	396.78	5.10	2413
384.25	5.10	2564	396.79	4.90	2352
384.28	4.90	2472	396.79	5.67	2661
395.14	7.00	4011	396.92	6.10	3032
395.80	0.90	1724	395.37	0.10	1708
395.83	6.10	3051	398.60	6.60	3273
396.07	7.82	4415	410.44	8.74	4159
396.16	7.69	4319	410.55	8.48	3960
396.25	7.50	4254	410.55	8.96	4200
396.27	7.40	4210	410.55	9.50	4421
396.29	7.20	4006	410.57	9.26	4352
396.55	0.90	1736	410.66	8.74	4110
396.73	4.84	2326	410.79	7.01	3093

presented in Fig. 2. The plots confirm the anomalous increase of the thermal conductivity in the vicinity of the critical point ( $T_c = 369.28$  K). Outside the region of the anomalous behavior, the error of the thermal-conductivity data did not exceed 2%. At temperatures and pressures where a critical enhancement in the thermal conductivity was observed, the error can be two or three times larger.

### 3. THERMAL CONDUCTIVITY OUTSIDE THE CRITICAL REGION

To represent the experimental thermal-conductivity data we have adopted an equation of the form

$$\lambda = \bar{\lambda} + \Delta_c \lambda \quad (1)$$

with

$$\bar{\lambda} = \lambda_0 + \Delta \lambda \quad (2)$$

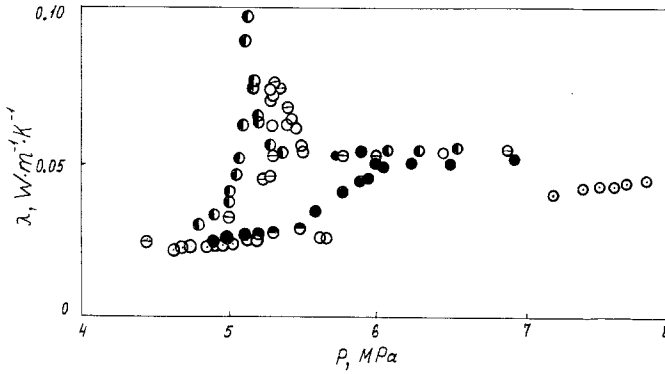


Fig. 2. Thermal conductivity of R22 as a function of pressures at various reduced temperatures.  $\tau = T/T_c$ :  $\bullet$   $\tau = 1.005$ ;  $\ominus$   $\tau = 1.011$ ;  $\bullet$   $\tau = 1.031$ ;  $\bullet$   $\tau = 1.073$ ;  $\circ$   $\tau = 1.112$ .

Here  $\bar{\lambda}$  is the regular or background thermal conductivity without anomalous critical contributions, while  $\Delta_c \lambda$  represents the additional enhancement of the thermal conductivity in the critical region. The thermal conductivity  $\bar{\lambda}$  is written as the sum of the thermal conductivity  $\lambda_0$  is the dilute-gas limit at the given temperature and an excess thermal conductivity  $\Delta \lambda$ . The critical temperature  $T_c$ , the critical pressure  $P_c$ , and the critical density  $\rho_c$  of R22 are

$$T_c = 369.28 \text{ K}, \quad P_c = 4.986 \text{ MPa}, \quad \rho_c = 512.82 \text{ kg} \cdot \text{m}^{-3} \quad (3)$$

The thermal conductivity is represented in terms of the reduced temperature  $\tau$  and the reduced density  $\omega$  defined as

$$\tau = T/T_c, \quad \omega = \rho/\rho_c \quad (4)$$

The thermal conductivity  $\lambda_0$  in the dilute-gas limit is represented by an equation similar to the one adopted earlier [9]

$$\lambda_0 = 0.01502 \phi(\tau) C_v^0(\tau)/C_v^0(\tau = 1) \quad (5)$$

where  $\lambda_0$  is in  $\text{W} \cdot \text{m}^{-1} \cdot \text{K}^{-1}$  and  $\phi(\tau)$  is a polynomial in terms of  $\tau$

$$\phi(\tau) = \sum_{i=0}^4 \phi_i \tau^i \quad (6)$$

while  $C_v^0$  is the ideal-gas specific heat which is represented by

$$C_v^0/J(\text{mol})^{-1} \text{ K}^{-1} = \sum_{i=0}^4 c_i \tau^i \quad (7)$$

**Table II.** Coefficients in Equations (6) and (7) for  $\lambda_0$ 

$i$	$\phi_i$	$c_i$
0	0.05342	15.5180
1	0.7256	36.0943
2	0.4612	15.0385
3	-0.2844	-15.1331
4	0.0449	3.2381

The values of the coefficients  $\phi_i$  and  $c_i$  are presented in Table II. Equation (5) represents the thermal conductivity in the dilute-gas limit to within about 2% in the temperature range from 230 to 500 K.

The excess thermal conductivity  $\Delta\lambda$  depends on the density alone at moderate gas densities, but shows an additional temperature dependence in the liquid phase. As in a previous publication [10] we represent the excess thermal conductivity  $\Delta\lambda$  in terms of a parameter  $s$  defined as

$$S = \omega\tau^{0.05} \quad (8)$$

In the range bounded by

$$0.31 < \tau < 1.23 \quad \text{and} \quad 0 < S < 3.1 \quad (9)$$

the excess thermal conductivity  $\Delta\lambda$  can be represented by

$$\Delta\lambda = \sum_{i=1}^6 b_i S^i \quad (10)$$

where  $\Delta\lambda$  is in  $\text{W} \cdot \text{m}^{-1} \cdot \text{K}^{-1}$ . The values of the coefficients  $b_i$  are given in Table III.

**Table III.** Coefficients in Equation (10) for  $\Delta\lambda$ 

$i$	$b_i$
1	$1.08109 \times 10^{-2}$
2	$3.14986 \times 10^{-2}$
3	$-2.93477 \times 10^{-2}$
4	$1.18373 \times 10^{-2}$
5	$-1.60394 \times 10^{-3}$
6	$6.618556 \times 10^{-5}$

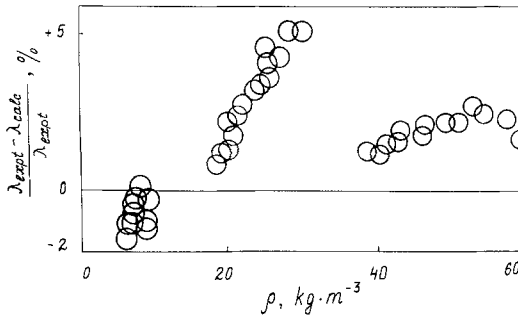


Fig. 3. Comparison of the thermal conductivity data of Gruzdjev et al. [11] with the values calculated from the recommended Eqs. (5) and (10).

An analysis of the thermal conductivity of R22 indicates that not all the sets of reported experimental data are equally reliable. There are regions where sizable discrepancies exist between measurements obtained with different methods. Figures 3–6 indicate the deviations of the experimental data from the values calculated with the recommended equations at densities and temperatures where the thermal conductivity may be identified with the regular thermal conductivity  $\bar{\lambda}$ .

#### 4. THERMAL CONDUCTIVITY IN THE CRITICAL REGION

Equation (2) with Eqs. (5) and (10) does not incorporate the anomalous behavior of the thermal conductivity in the vicinity of the critical point. Figure 7 shows the critical thermal-conductivity enhancement

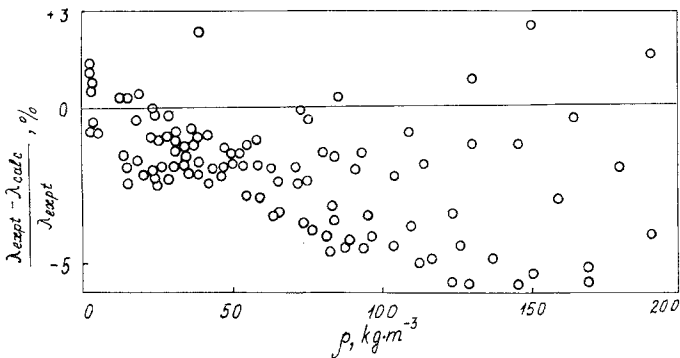


Fig. 4. Comparison of the thermal conductivity data of Makita et al. [4] with the values calculated from the recommended Eqs. (5) and (10).

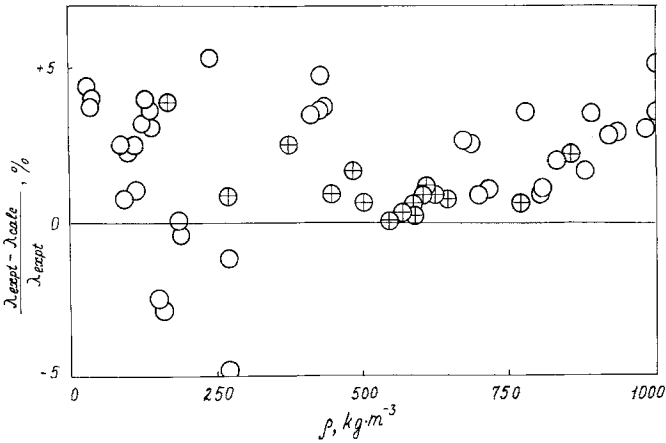


Fig. 5. Comparison of the thermal conductivity data of Geller et al. [12] with the values calculated from the recommended Eqs. (5) and (10): ○, Geller et al. [12]; ⊕, Geller [5].

$\Delta_c \lambda$  at  $\rho = \rho_c$  as a function of  $\Delta T = T - T_c$  on a double-logarithmic scale. Close to the critical temperature these data are represented by a power law of the form [13]

$$\Delta_c \lambda(\rho_c, T) = D \varepsilon^{-\psi} \quad (11)$$

with  $\varepsilon = \tau - 1$ . The parameters  $D$  and  $\psi$  were fitted to the experimental data with the results  $D = 196 \times 10^{-5} \text{ W} \cdot \text{m}^{-1} \cdot \text{K}^{-1}$  and  $\psi = 0.633$ . From Fig. 7 we note that at temperatures above  $T = 396 \text{ K}$  the experimentally observed

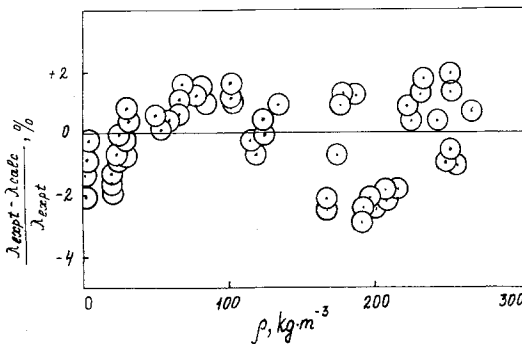


Fig. 6. Comparison of the thermal conductivity data obtained with our apparatus with those calculated from the recommended Eqs. (5) and (10).



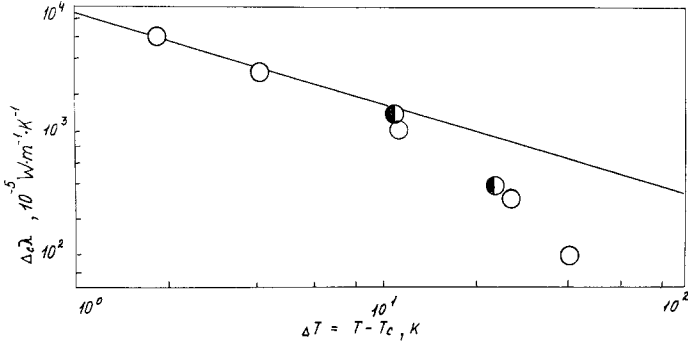


Fig. 7. The critical thermal conductivity enhancement at  $\rho = \rho_c$  as a function of  $\Delta T = T - T_c$ : ○, the present study; ●, Geller [5].

$\Delta_c \lambda$  is less than the value implied by the asymptotic power law (11). It should be noted that our results are in a rather good agreement with those of Geller [5] except at  $T = 380.18$  K, where the value found by Geller is somewhat larger.

We represent the critical thermal-conductivity enhancement by an equation developed by Sengers [13]:

$$\Delta_c \lambda = \frac{k_B T^2}{6\pi\eta\xi} \left( \frac{\partial P}{\partial T} \right)_v K_T F \quad (12)$$

where  $k_B$  is the Boltzmann constant,  $\eta$  the shear viscosity,  $K_T$  the isothermal compressibility,  $\xi$  the correlation length, and the function  $F$  is given by

$$F = \exp[-\{A(\tau - 1)^2 + B(\omega - 1)^4\}] \quad (13)$$

An equation of this form was originally proposed by Hanley et al. [14].

From our thermal-conductivity measurements, it was found that  $A = 45.0$  and  $B = 6.0$ .

For the present study, we estimated the correlation length from an approximate relationship [13] as

$$\xi = \xi_0 \sqrt{nk_B T K_T} \quad (14)$$

where  $n$  is the number density. In the case of R22 we define  $\xi_0$  by an equation proposed by Hanley et al. [15]:

$$\xi_0 = A_0 \left( \frac{\omega}{\tau} \right)^{1/2} \quad (15)$$

In the absence of light-scattering data we imposed for R22 the value  $A_0 = 4.0 \text{ \AA}$ .

For the calculation in the range  $(\omega - 1) \leq 0.25$  and  $(\tau - 1) \leq 0.03$ , the values of  $K_T$  were determined with the equation given by Levelt Sengers et al. [16].

$$\omega^2 K_T P_c = (\omega - 1)^{1-\delta} \left[ \delta h(X) - \frac{X}{\beta} \frac{dh(X)}{dX} \right]^{-1} \quad (16)$$

where

$$h(X) = E_1 \theta (1 + E_2 \theta^{2\beta})^{(\gamma-1)/2\beta} \quad (17)$$

and

$$\theta = 1 + \frac{X_0}{X} \quad (18)$$

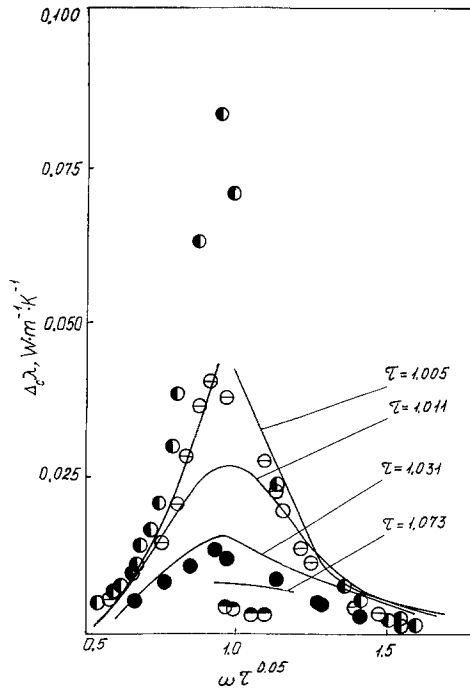


**Fig. 8.** The critical thermal conductivity enhancement data for R22 in the critical region as a function of density along isotherms. The data are those obtained with our apparatus and the curves represent the values calculated from Eq. (12):  $\bullet$   $\tau = 1.005$ ;  $\ominus$   $\tau = 1.011$ ;  $\circ$   $\tau = 1.031$ ;  $\bullet$   $\tau = 1.073$ .

while the functions  $X$  and  $X_0$  are given by

$$X = (\tau - 1)/|(\omega - 1)|^{1/\beta} \quad (19)$$

and

$$|X_0| = B_0^{-1/\beta} \quad (20)$$

The R22 density data on the coexistence curve [17] allowed us to derive  $B_0 = 2.034$  and  $\beta = 0.35$ . We have adopted  $E_1 = 2.03$  for methane and  $E_2 = 0.237$  as the universal value [16]. For the universal critical exponents  $\gamma$  and  $\delta$  we have adopted the values  $\gamma = 1.243$  and  $\delta = 4.656$ . The calculations of  $K_T$  in the range  $(\omega - 1) > 0.25$  and  $(\tau - 1) > 0.03$  were done according to the analytical equation of state [17].

In Fig. 8 we represent a comparison between our experimental  $\Delta_c \lambda$  data and the thermal-conductivity enhancements calculated from the mode coupling theory approximation (12). It can be seen that the experimental and predicted data do not coincide in full, but considering the singular behavior of the thermodynamic properties involved in the plot, this degree of agreement is remarkable and confirms the validity of Eq. (12).

In addition, we developed here an empirical relationship to calculate the singular thermal conductivity  $\Delta_c \lambda$  as

$$\Delta_c \lambda = (S^{0.5}/D) \exp(-bz^{0.6}) \quad (21)$$

This model implies the following functions of  $S = \omega\tau^{0.05}$ ,  $(\tau - 1)$ , and  $(\omega - 1)$ :

$$Z = (S - S_{\max})^2 \quad (22)$$

$$D = C + d|\tau - 1| + \sum_{i=2}^4 f_i \exp\left(-\frac{\alpha_i}{|\tau - 1|^i}\right) \quad (23)$$

**Table IV.** Coefficients in Equations (23), (24), and (25) for  $\Delta_c \lambda$ .

$i$	$f_i$	$\alpha_i$	$h_i$	$g_i$	$\beta_i$
0	—	—	$1.12573 \times 10^1$	—	—
1	—	—	$-7.25334 \times 10^2$	—	—
2	$1.95830 \times 10^{-4}$	$9.35880 \times 10^{-4}$	$2.72652 \times 10^4$	5.63240	$-9.36060 \times 10^{-6}$
3	$2.54296 \times 10^{-3}$	$3.08966 \times 10^{-4}$	$-3.74741 \times 10^5$	$-4.43102 \times 10^{-1}$	$8.33710 \times 10^{-6}$
4	$3.16124 \times 10^{-2}$	$3.57666 \times 10^{-4}$	$1.64692 \times 10^6$	$-7.47689 \times 10^{-1}$	$6.29683 \times 10^{-6}$

where  $S_{\max} = 0.95$ ,  $C = 1.894 \times 10^{-5}$ , and  $d = 1.894 \times 10^{-2}$ . We have adopted

$$b = \sum_{i=0}^4 h_i |\tau - 1|^i \quad \text{for } |\tau - 1| \leq 0.005 \quad (24)$$

and

$$b = \sum_{i=2}^4 g_i \exp\left(-\frac{\beta_i}{|\tau - 1|^i}\right) \quad \text{for } |\tau - 1| > 0.005 \quad (25)$$

The values of the coefficients  $h_i$ ,  $f_i$ ,  $\alpha_i$ ,  $g_i$ , and  $\beta_i$  are presented in Table IV. The maximum deviations of our experimental  $\Delta_c \lambda$  from empirical Eq. (21) are 12% near the critical point.

In Table V we show a comparison between the values calculated from Eq. (21) for the thermal conductivity of  $\text{CO}_2$  in the critical region and the experimental data of Sengers [7, 18]. The equation yields a reasonable representation of the thermal conductivity in the critical region, for  $S_{\max} = 1.0$  in Eq. (22).

**Table V.** Thermal Conductivity of  $\text{CO}_2$  Calculated from the Recommended Interpolating Equations

$10^5(\Delta_c \lambda) (\text{W} \cdot \text{m}^{-1} \cdot \text{K}^{-1})$				
$\omega$	$T - T_c = 0.20 \text{ K}$		$T - T_c = 1.10 \text{ K}$	
	Experimental [18]	Calculated	Experimental [18]	Calculated
0.7173	3640	2523	3180	1353
0.8017	5900	6063	4900	2831
0.8439	7980	9153	6090	4004
0.8861	11500	13523	7440	5562
0.9283	18900	19436	8820	7547
0.9705	26700	26804	9570	9896
1.0127	28200	30277	9310	10965
1.0549	23000	23490	8200	8906
1.0970	13200	17297	6670	6931
1.1392	7520	12345	5250	5250
1.2236	3950	5890	3320	2850
1.3080	2400	2635	2180	1470

## REFERENCES

1. N. B. Vargaftik, L. P. Filippov, A. A. Tarzimanov, and E. E. Totksiy, *Thermal Conductivity of Gases and Liquids* (Izd. Standarty, Moscow, 1978).
2. V. V. Altunin, V. Z. Geller, E. K. Petrov, D. S. Rasskazov, and G. A. Spiridonov, *Thermophysical Properties of Freons, Vol. 1. Freons of the Methane Row*, S. L. Rivkin, ed. (Izd. Standarty, Moscow, 1980).
3. O. B. Tsvetkov, Y. S. Tchilipyonok, and G. N. Danilova, *Kholodil'naya Tekhnika* **12**:17 (1976).
4. T. Makita, Y. Tanaka, Y. Morimoto, M. Noguchi, and H. Kubota, *Int. J. Thermophys.* **2**:249 (1981).
5. V. Z. Geller, *Thermophysical Properties of Substances and Materials, Issue 22* (GSSSD, Moscow, 1985), p. 101.
6. O. B. Tsvetkov and Y. A. Laptyev, *Kholodil'naya Tekhnika* **6**:60 (1982).
7. J. V. Sengers, *Thermal Conductivity Measurements at Elevated Gas Densities Including the Critical Region* (Van Gorcum, Assen, The Netherlands, 1962).
8. A. Michels, J. V. Sengers, and P. S. van der Gulik, *Physica* **28**:1201 (1962).
9. O. B. Tsvetkov, *J. Phys. Eng.* **42**:955 (1982).
10. O. B. Tsvetkov, Ref. 5, p. 118.
11. V. A. Gruzdyev, A. I. Shestova, and V. V. Selin, *Thermophysical Properties of Freon* (Novosibirsk, 1974).
12. V. Z. Geller, S. I. Ivantchenko, and V. Z. Peredriy, *Izvest. VUZOV, Neft i Gas* **8**:61 (1973).
13. J. V. Sengers, *Int. J. Thermophys.* **3**:203 (1985).
14. H. J. M. Hanley, J. V. Sengers, and J. F. Ely, in *Thermal Conductivity 14*, P. G. Klemens and T. K. Chu, eds. (Plenum, New York, 1976), p. 383.
15. H. J. M. Hanley, R. D. McCarty, and J. V. Sengers, *NASA CR-2440* (NASA, Washington, D.C., 1974).
16. Y. M. H. Levelt Sengers, W. L. Greer, and J. V. Sengers, *J. Phys. Chem. Ref. Data* **5**:1 (1976).
17. A. V. Kletskiy, *Tables of Thermodynamic Properties of Gases and Liquids, Issue 2, Freon-22* (Izd. Standarty, Moscow, 1978).
18. J. V. Sengers, *Ber. Bunsenges. Phys. Chem.* **76**:234 (1972).